ROYAL SOCIETY OF CHEMISTRY

PAPER

Simultaneous measurement stable and radiogenic Nd isotopic compositions by MC-ICP-MS with a single-step chromatographic extraction technique†

Jiang-Hao Bai, [ID] ‡[abg] Fang Liu,‡*[d] Zhao-Feng Zhang, [ID] [d] Jin-Long Ma, [ID] [ab] Le Zhang, [ID] [ab] Yu-Fei Liu,[e] Song-Xiong Zhong[f] and Gang-Jian Wei [ID] *[abc]

Removing interferences such as Ce on Nd isotopes during column chemistry is hard to achieve due to their similar properties. In this study, we established a simple but efficient Nd separation technique with the perfect separation of Nd from Ce and nearly 100% Nd yield using the TODGA resin (50–100 μm, Eichrom, USA) after actual measurements. All samples used here through the Nd separation technique have Ce/Nd ratios less than 0.003. The whole procedure takes about 10 h. The stable Nd isotopes were measured by MC-ICP-MS and calibrated with standard-sample-standard bracketing (SSB) combined Eu internal normalization. The potential influences of Eu and Ce on stable Nd isotopic analysis were strictly evaluated. The long-term analyses of the JNdi-1 standard produced a total average $\delta^{142/144}$Nd of 0.000 ± 0.029‰ (2SD, $n = 210$), $\delta^{145/144}$Nd of 0.000 ± 0.029‰ (2SD, $n = 210$), and $\delta^{146/144}$Nd of 0.000 ± 0.027‰ (2SD, $n = 210$). Two pure Nd standards, La Jolla and Nd-GIG, produced $\delta^{146/144}$Nd values (means ± 2SD, $n = 20$) of −0.227 ± 0.030‰ and 0.226 ± 0.021‰, respectively. $\delta^{146/144}$Nd (means ± 2SD, $n = 20$) of seven geological reference materials (BCR-1, BHVO-2, AGV-2, GSP-2, NOD-P-1, NOD-A-1, and GBW07249) were also reported. The reproducibility of $\delta^{146/144}$Nd was better than 0.030‰. These results are in good agreement with the published DS-TIMS methods. In addition, our method also allows the concurrent determination of the radiogenic ^{143}Nd/^{144}Nd ratio. All the ^{143}Nd/^{144}Nd ratios of these samples are identical with the preferred values published in the GeoReM Database. These results indicated that the method of Nd isotopic analysis established here can simultaneously measure high-precision $\delta^{142/144}$Nd, $\delta^{145/144}$Nd, $\delta^{146/144}$Nd, and radiogenic ^{143}Nd/^{144}Nd ratio for geological materials.

1. Introduction

Neodymium (Nd) is a highly incompatible, refractory rare earth element (REE), which plays a crucial role in geological processes. It has seven isotopes with a nominal mass of 142, 143, 144, 145, 146, 148, and 150, and typical abundances of 27.152%, 12.174%, 23.798%, 8.293%, 17.189%, 5.756%, and 5.638%, respectively.[1] The variations in the Nd isotopic ratios can be caused by mass-independent and mass-dependent effects. The former includes the decay of ^{147}Sm to ^{143}Nd and ^{146}Sm to ^{142}Nd, nucleosynthetic anomaly, as well as any physical mass-independent fractionation. The latter describes the stable Nd isotopic compositions, which is the atomic mass difference related to natural isotopic fractionation. The mass-independent Nd isotopic effects have been extensively used as geological chronometers and tracers in Earth and planetary differentiation,[2–6] petrogenetic studies,[2] climate change,[7] and ocean circulation.[8,9] In contrast, the stable Nd isotope geochemistry is

[a]*State Key Laboratory of Isotope Geochemistry, Guangzhou Institute of Geochemistry, Chinese Academy of Sciences, Guangzhou 510640, China. E-mail: gjwei@gig.ac.cn*

[b]*CAS Center for Excellence in Deep Earth Science, Guangzhou 510640, China*

[c]*Southern Marine Science and Engineering Guangdong Laboratory, Guangzhou 511458, China*

[d]*International Research Center for Planetary Science, College of Earth Sciences, Chengdu University of Technology, Chengdu 610059, China. E-mail: liufang@cdut.edu.cn*

[e]*Guangzhou Marine Geological Survey, China Geological Survey, Guangzhou 510075, China*

[f]*National-Regional Joint Engineering Research Center for Soil Pollution Control and Remediation in South China, Guangdong, Key Laboratory of Integrated Agro-environmental Pollution Control and Management, Institute of Eco-environmental and Soil Sciences, Guangdong Academy of Sciences, Guangzhou 510650, China*

[g]*University of Chinese Academy of Sciences, Beijing 100049, China*

† Electronic supplementary information (ESI) available. See DOI: 10.1039/d1ja00302j

‡ These authors contributed equally to this work.

in its infancy. The currently available data[10–14] have shown significant stable Nd isotopic fractionations (up to 0.160‰) during geological processes. For this reason, the stable Nd isotopes can provide new constraints in a diverse range of geological processes described above.

The double spike-thermal ionization mass spectrometry (DS-TIMS) technique was the preferred method for stable Nd isotopic analysis.[10,15,16] This technique is well known for its high precision without the need of 100% yield but is time-consuming for preparing samples and is complicated in calculation. Rather, the MC-ICP-MS method offers a more convenient way and comparable precision to that of DS-TIMS. This method, however, requires 100% Nd recovery and perfect Ce–Nd, Pr–Nd, and Sm–Nd separation, and has much larger instrumental mass bias. Previous studies showed that even trace amounts of Ce could cause significant bias on the $\delta^{142/144}$Nd value.[13,17] Therefore, stable Nd isotopic compositions measured by MC-ICP-MS have higher requirements for Nd purification in column chemistry.

The conventional extraction chromatography protocols of radiogenic Nd isotope are not applicable to the separation of stable Nd isotopes because of its difficulty in recovering nearly 100% of Nd and perfectly separating Nd from Ce. To account for this, several studies have tried to develop stable Nd isotope analytical procedures.[10,13,15–19] For example, to eliminate the matrix elements such as Ca and Mg, and isobaric elements such as Ce and Sm, the purification of Nd is commonly performed using one-,[17] two-,[10,13,15] three-,[19–21] or even four-stage[18,22] chemical separation procedures (Table S1†). Multi-step chemical purifications are laborious, time-consuming, and lead to high total procedural blank. Besides, the conventional Ln resin cannot achieve the complete separation of Nd from Ce and Pr because of the small difference in the distribution coefficients of these elements.[17] Recently, the TODGA resin was also introduced for Nd purification.[17,23,24] For example, Wang, et al.[17] successfully purified Nd by a single TODGA column purchased by TrisKem International. However, their method applied 2.3 M HCl elution to remove Ca together with La, Ce, and Pr, which may cause minor residual Ca in the Nd fraction for high Ca content samples.[24] More importantly, the perfect separation of Nd from Ce has not been well established so far.

In this study, we developed a novel chemical purification of Nd through a single TODGA resin column (Eichrom industry, USA), obtaining pure Nd fractions free of Ce, Pr, as well as Sm, and nearly 100% Nd yield. Due to the excellent chemical procedures, we can simultaneously achieve measurements of stable and radiogenic Nd isotopic compositions by MC-ICP-MS. In addition, standard-sample bracketing combined with Eu as an internal standard was employed to calibrate the mass discrimination for stable Nd isotopic analysis, which increases the precision up to 3-folds than the SSB method alone. The feasibility of our method was verified by the determination of three pure Nd standards and seven geological reference materials.

2. Experimental section

2.1 Reagents and materials

Nitric acid (HNO_3), hydrochloric acid (HCl), and hydrofluoric acid (HF) (Beijing Institute of Chemical Reagents, China) were purified by double sub-boiling distillation in Savillex DST-1000 system (USA). Ultra-pure water with a resistivity of 18.2 MΩ cm was obtained from a Millipore system (USA). The exchange column with 6 cm length and 0.7 cm diameter was manufactured by the Bio-Rad company (USA). The TODGA resin with 50–100 μm particle size was made in the Eichrom Industry, single element solutions of Mg, Fe, Al, Ca, K, Na, Mn, Ti, Ba, Sr, Pb, U, and rare earth elements (REEs) in the Beijing General Research Institute for Nonferrous Metals (BGRINM, China), and JNdi-1 in the Geological Survey of Japan. The pure Eu single solution (1000 μg g^{-1}) from BGRINM was also used as an internal standard in this study. The Eu single solution was diluted to 50 ng g^{-1} with 2% HNO_3 and was then scanned for the ^{140}Ce and ^{144}Nd signal by MC-ICP-MS. The results show the intensity of both ^{140}Ce and ^{144}Nd less than 0.1 mV. In addition to these standard materials, our laboratory in-house standard (Nd-GIG, Nd_2O_3) was also analyzed. This could be very useful for comparisons of the Nd isotopic results calculated against different Nd standards and different laboratories.

A series of geological rocks including BCR-1, BHVO-2, AGV-2, GSP-2, NOD-P-1, NOD-A-1, and GBW07249 were selected for stable and radiogenic Nd isotopic analysis. These rock samples cover a wide range of rock types from basaltic and felsic to sedimentary rocks, allowing us to evaluate the efficiency of chemical purification.

2.2 Chemical purification

2.2.1 Sample digestion. All chemical procedures were carried out in a class 100 hood at the State Key Laboratory of Isotope Geochemistry, Guangzhou Institute of Geochemistry, Chinese Academy of Sciences (SKLBIG-GIGCAS). Approximately 4 to 40 mg of the sample powders, depending on the Nd contents, were weighed into PFA Savillex beakers. After the addition of a 3 : 1 mixture of concentrated HF–HNO_3 into the samples, the container was heated on a hot plate at 120 °C for 5 days. The sample solutions were then evaporated to dryness at 100 °C and redissolved in 2 mL 6 M HCl to remove residual fluorides. Once in clear solutions, the samples were dried and

Table 1 Nd purification procedure on a single TODGA resin column

Eluents	Volume/mL	Step
0.1 M HCl	20	Cleaning
Milli-Q H_2O	5	Cleaning
2 M HNO_3	3 + 3	Conditioning
2 M HNO_3	0.5	Loading
2 M HNO_3	4.5	Remove Na, Mg, Al, Ti, Ba, Fe, Mn, K, Rb
8 M HNO_3	15	Remove Pb, Sr, Ca
2.6 M HCl	26	Remove La, Ce, Pr
2 M HCl	12	Collect Nd
0.1 M HCl	20	Remove other REEs and U

2696 | J. Anal. At. Spectrom., 2021, **36**, 2695–2703

This journal is © The Royal Society of Chemistry 2021

dissolved in 0.5 mL 2 M HNO_3 for chromatographic column chemistry.

2.2.2 Column chemistry. The procedures of Nd purification are listed in Table 1. Briefly, Nd purification was performed in Bio-Rad columns loaded with 2 mL of Eichrom TODGA resin. The resin-filled columns were cleaned with 5 mL Milli-Q H_2O and 20 mL 0.1 M HCl, and then conditioned twice with 3 mL 2 M HNO_3. 0.5 mL 2 M HNO_3 of the sample solutions containing 1 µg Nd was loaded into the resin. Then, 4.5 mL 2 M HNO_3 was used to elute the matrix elements including Mn, Ti, Fe, Al, Mg, K, Na, Ba, and Rb, and 15 mL 8 M HNO_3 was used to elute Pb, Sr, and Ca. Subsequently, La, Ce, and Pr were eluted by 26 mL 2.6 M HCl, and Nd was collected with 12 mL 2 M HCl in pre-cleaned Teflon beakers. Finally, the residual REEs and U were removed using 20 mL 0.1 M HCl. The pre-cut and post-cut aliquots were collected in 4 mL tubes to check the Nd yield using inductively coupled plasma mass spectrometry (ICP-MS). The yields of these geological samples analyzed here are above $99.5 \pm 0.5\%$ ($n = 7$). The whole procedure can be finished in ~10 h.

2.3 MC-ICP-MS measurement

2.3.1 Instrumentation. Stable and radiogenic Nd isotopic ratios were determined on a ThermoFisher Scientific Neptune Plus MC-ICP-MS at the SKLBIG-GIGCAS. The instrument is equipped with 9 Faraday cups, 8 of which are used in our measurement. The cups L4, L3, L2, L1, C, H1, H2, and H3 were used to collect ^{140}Ce, ^{142}Nd, ^{143}Nd, ^{144}Nd, ^{145}Nd, ^{146}Nd, ^{151}Eu, and ^{153}Eu, simultaneously. Unfortunately, the unavailable axial Faraday cup was assigned to ^{148}Nd or ^{150}Nd. If we chose ^{148}Nd or ^{150}Nd, our machine would not be able to measure the ratio of $^{153}Eu/^{151}Eu$. We therefore gave up the measurement of ^{148}Nd and ^{150}Nd. ^{140}Ce was used to examine the isobaric interference of ^{142}Ce on ^{142}Nd using $^{142}Ce = 0.12589 \times {}^{140}Ce$.[25] Combined standard sample bracketing and Eu internal normalization

isotopic fractionation correction technique was employed to improve the reproducibility of the stable Nd isotopic analysis. For the measurement of the radiogenic $^{143}Nd/^{144}Nd$ ratio, the $^{146}Nd/^{144}Nd$ ratio of 0.7219 was used to correct the mass bias. Each analysis consisted of 60 cycles of data with an integration time of 4.194 s. All measurements were carried out in low resolution model using a wet sample introducing system with a Micromist PFA nebulizer and a glass cyclonic spray chamber. The analyses were repeated more than 4 times for the same analyte solution. During the experiment, 2% HNO_3 was used through the total procedure including the dilution of the analyte and the washing of the sample introduction system to avoid the potential effect of acid molarity.[26,27] The typical sensitivity of ^{144}Nd was 17.5 V per µg g^{-1}, and the mass fractions of Nd solutions were 200 ng g^{-1}. To eliminate the cross-contamination between the analyte and the standard, the washing time was set to about 4 minutes and the background of ^{144}Nd was less than 0.2 mV. Other instrumental parameters are listed in Table 2.

2.3.2 Combined standard-sample bracketing and internal normalization (C-SSBIN) isotopic fractionation correction for stable Nd isotopic analysis. The mass discrimination effect is an inevitable feature of mass spectrometers, in particular, for MC-ICP-MS instruments due to its space charge ion dispersion in the plasma or vacuum interference region.[19,28–30] For Nd isotopes, the previous works have shown that the typical mass-discrimination effect in MC-ICP-MS was about 1.4% per amu.[31] In order to accurately correct this effect, sample standard bracketing and Eu internal correction were combined for stable Nd isotopic analysis in this work.

The SSB model is based on the sequential measurements of standard-sample-standard, and is efficient for providing the accuracy of isotopic analysis. As reported by previous studies, this model has been widely applied to most metal stable isotope measurements.[29,32–35] However, the prerequisite of SSB is that

Table 2 Instrumental operating parameters for stable and radiogenic Nd isotope measurements

Instrument parameters	Neptune plus
RF power	1098 W
Cooling gas	16.7 L min^{-1}
Auxiliary gas	1.0 L min^{-1}
Sample gas	1.0 L min^{-1}
Extraction	−2000 V
Focus	−726 V
Data acquisition (integration × cycle × block)	4.194 s per cycle × 60 cycle × 1
Typical ^{144}Nd sensitivity	17.5 V ppm^{-1}
Background of ^{144}Nd	Less than 0.2 mV
Mass resolution	Low resolution
Sample uptake	50 µL min^{-1}
Spray chamber	Glass cyclonic
Nebulizer type	Micromist PFA nebulizer
Mass bias correction	Internal correction using $^{153}Eu/^{151}Eu = 1.09160$ (ref. 19 and 40)

Cup	L4	L3	L2	L1	C	H1	H2	H3
	^{140}Ce	^{142}Nd	^{143}Nd	^{144}Nd	^{145}Nd	^{146}Nd	^{151}Eu	^{153}Eu

This journal is © The Royal Society of Chemistry 2021

J. Anal. At. Spectrom., 2021, **36**, 2695–2703 | **2697**

the mass discriminations between the samples and the standards are identical, which may be problematic in actual samples because of the varying matrix influences among different sample types. On the other hand, this approach cannot monitor the short-term drift of mass bias between bracketing standards. These deficits of the SSB method can be well compensated for using internal normalization.[30]

Internal normalization model adopts a known isotope ratio of the standard to calibrate the isotope ratio of the target element based on the mass-dependent fractionation laws. This method has been applied for several isotope analyses, such as Fe–Cu,[36] Mo–Zr–Ru,[37] and Pb–Tl.[38] The principle behind selecting a calibrator is the closeness to the target element in mass and not cause isobaric interferences.[30] For Nd isotope analysis, Eu is the most suitable calibrator because of the isobaric interference of Ce and Sm as well as the large difference between ^{138}La (0.09%) and ^{139}La (99.91%).

According to the exponential calibration model, the fractionation factor of Eu isotopes denoted as f_{Eu} can be obtained as below.

$$f_{Eu} = \ln\left(\frac{\left(^{153}Eu/^{151}Eu\right)_T}{\left(^{153}Eu/^{151}Eu\right)_M}\right) \Big/ \ln\left(\frac{m153}{m151}\right) \quad (1)$$

where m represents the absolute masses of the isotopes of interest, $m151 = 150.91986$, $m153 = 152.92124$,[39] subscript T and M is the true and measured values, respectively. The ratio of $\left(^{153}Eu/^{151}Eu\right)_T$ is 1.09160.[19,40] In principle, Eu and Nd have a very close mass number, from which it can be assumed that the fractionation behavior is the same in MC-ICP-MS. Based on f_{Eu}, the true Nd isotopic ratio can be calculated as follows.

$$\left(\frac{^X Nd}{^{144}Nd}\right)_T = \left(\frac{^X Nd}{^{144}Nd}\right)_M \times \left(\frac{mX}{m144}\right)^{f_{Eu}} \quad (2)$$

where x is 142, 145, and 146, $m142 = 141.90773$, $m144 = 143.91008$, $m145 = 144.91258$, and $m146 = 145.91313$.[39] The stable Nd isotopic compositions can thus be calculated from the corrected Nd isotope ratios of the sample and the averages of the bracketing JNdi-1 as follows.

$$\delta^X Nd = \left[\frac{2 \times \left(^X Nd/^{144}Nd_{sample}\right)C}{\left(^X Nd/^{144}Nd_{JNdi-1A}\right)C + \left(^X Nd/^{144}Nd_{JNdi-1B}\right)C} - 1\right] \times 1000 \quad (3)$$

where JNdi-1A and JNdi-1B refer to the JNdi-1 standard measured before and after the sample, respectively. The subscript C is the correction value using the ratio of $\left(^{153}Eu/^{151}Eu\right)_T$. For radiogenic $^{143}Nd/^{144}Nd$ measurements, it is often reported in traditional ε values or normalized $^{143}Nd/^{144}Nd$ ratios using $^{146}Nd/^{144}Nd = 0.7219$ by the exponential law.

3. Results and discussion

3.1 The elution curves of Nd and its effectiveness

To establish the separation protocol to purify Nd for isotopic analysis on MC-ICP-MS, the elution behavior of the target
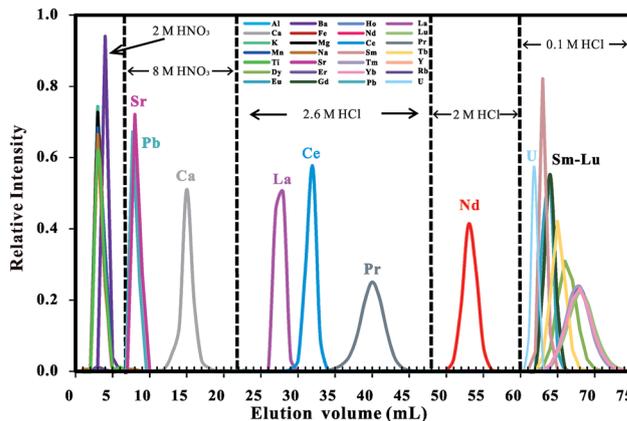

Fig. 1 Elution curves of Nd purification procedures using a synthetic solution (Mg : Fe : Al : Ca : K : Na : Mn : Ti : Ba : Sr : Rb : Pb : U : REEs = 12 : 12 : 12 : 12 : 7 : 7 : 5 : 5 : 3 : 3 : 2 : 1 : 1 : 1) on a 2 mL TODGA resin column.

element Nd, the matrix elements (e.g., Ca), and isobaric elements (e.g., Ce) in 2 mL Eichrom TODGA resin was thoroughly investigated. A synthetic solution was the first tested elution curve. The elution was continuously collected every 1 mL, and was measured for Al, Ba, Ca, Fe, K, Mg, Mn, Na, Ti, Sr, and Rb by ICP-AES at SKLBIG-GIGCAS, and other trace elements including Pb, U, and REEs were analyzed with an ThermoFisher Scientific X series 2 inductively coupled plasma mass spectrometry (ICP-MS) at Guangzhou Marine Geological Survey, China Geological Survey. The proportion of each element relative to its total loading was calculated to construct the elution curves (Fig. 1). As shown in Fig. 1, the matrix elements of Fe, Mn, Ti, Al, Mg, K, Na, Ba, and Rb were completely eluted using 5 mL 2 M HNO_3 in 2 mL Eichrom TODGA resin. However, 10 mL 3 M HNO_3 (ref. 17 and 24) or 6 mL 2 M HNO_3 (ref. 23) was adopted as the eluent for 1 mL TrisKem TODGA resin. Pb and Sr have similar affinity to the TODGA resin.[41] Their ability increased when the molarity of HNO_3 < 1 M and then decreased to no absorption in >4 M HNO_3. Therefore, 4 M HNO_3 (ref. 35) or 6 M HNO_3 (ref. 42) was used to remove Sr. For Ca, Wang et al.[17] applied 2.3 M HCl to elute Ca together with La, Ce, and Pr, which may cause minor residual Ca tailing into the Nd fraction for the samples of high Ca content. For this reason, Chu et al.[24] added a 10 mL 11 M HNO_3 elution step after the 10 mL 3 M HNO_3 stage to remove Ca. Retzmann et al.[23] used 10 mL 0.1 M HNO_3 to remove Ca. 15 mL 8 M HNO_3 were used in this study to remove Pb, Sr, and Ca. The ability of U and Sm–Lu to be retained in the TODGA resin rapidly decreased as the molarity of HCl decreased.[41] Therefore, 0.1 M HCl was used here. Moreover, previous studies show a larger proportion of residual Ce in Nd cut than that in our methods (see Table S1†). This is likely due to the difference between TrisKem and Eichrom.

The effectiveness of the elution curves was evaluated in the following procedures. First, JNdi-1 including 1 μg Nd was loaded in the columns and then measured by MC-ICP-MS. Its result, expressed as $\delta^{146/144}Nd_{processed}$ value, is in good agreement with the result without column chemistry, which is denoted as $\delta^{146/144}Nd_{without\ processed}$ value (Table 3). This

Table 3 Stable and radiogenic Nd isotopic compositions of pure Nd standards and rock standards[a]

Sample ID	Nd (ppm)	$^{140}Ce/^{144}Nd$	$(^{143}Nd/^{144}Nd)_N$	$\delta^{142/144}Nd$	2SD	$\delta^{145/144}Nd$	2SD	$\delta^{146/144}Nd$	2SD	n	Ref.
Processed JNdi-1		2.94×10^{-5}	0.512104 ± 8	−0.003	0.029	−0.006	0.031	−0.007	0.021	6	This study
La Jolla		3.41×10^{-5}	0.511856 ± 11	0.230	0.029	−0.114	0.025	−0.227	0.030	20	This study
						−0.122	0.020	−0.243*	0.040*	3	Saji *et al.* (2016)[18]
								−0.214	0.010	7	McCoy-West *et al.* (2020a)[16]
				0.210	0.020	−0.110	0.011	−0.206	0.017	13	Ma *et al.* (2013)[13]
			0.511849	0.211	0.018	−0.100	0.090	−0.197	0.023	2	Wakaki and Tanaka, (2012)[15]
Nd-GIG		1.66×10^{-5}	0.511512 ± 9	−0.237	0.025	0.105	0.030	0.226	0.021	20	This study
				−0.233	0.019	−1.000	0.009	0.225	0.020	13	Ma *et al.* (2013)[13]
BCR-1	29	2.40×10^{-3}	0.512609 ± 11	0.033	0.010	−0.007	0.020	−0.022	0.030	4	This study
								−0.023	0.016	3	McCoy-West *et al.* (2017)[10]
BHVO-2	24.5	1.90×10^{-3}	0.512987 ± 17	0.025	0.045	−0.008	0.031	−0.030	0.030	4	This study
								−0.030	0.014	6	McCoy-West *et al.* (2020a)[16]
						0.000	0.030	0.000*	0.030	3	Pin and Gannoun, (2019)[20]
				0.018	0.033			−0.018	0.033	21	Wang *et al.* (2017)[17]
				0.098	0.018	−0.059	0.012	−0.072	0.010	5	Ma *et al.* (2013)[13]
						−0.030	0.020	−0.060*	0.040	5	Saji *et al.* (2016)[18]
AGV-2	30.5	2.61×10^{-3}	0.512786 ± 10	0.010	0.020	0.004	0.040	−0.014	0.030	4	This study
				0.016	0.029			−0.016*	0.029	20	Wang *et al.* (2017)[17]
GSP-2	207.3	2.59×10^{-3}	0.511361 ± 9	0.054	0.037	−0.028	0.028	−0.063	0.031	4	This study
				0.085	0.010	−0.042	0.008	−0.071	0.009	2	Ma *et al.* (2013)[13]
						−0.020	0.006	−0.040*	0.012	5	Saji *et al.* (2016)[18]
NOD-P-1	127.8	2.62×10^{-3}	0.512432 ± 14	0.024	0.033	−0.004	0.029	0.002	0.026	4	This study
NOD-A-1	98.8	9.67×10^{-3}	0.512136 ± 5	0.055	0.052	−0.007	0.021	−0.015	0.028	4	This study
GBW07249	238	5.23×10^{-3}	0.512334 ± 12	0.044	0.036	−0.018	0.010	−0.030	0.023	4	This study

[a] n is the times of repeated measurements of the same solution. 2SD = 2 times the standard deviation of the population of n repeat measurements. *represents $\delta^{146/144}Nd$ values corrected to $\delta^{146/144}Nd = -0.9865 \times \delta^{142/144}Nd$ and $\delta^{146/144}Nd = 1.9912 \times \delta^{145/144}Nd$ using the exponential fractionation laws. The $(^{143}Nd/^{144}Nd)_N$ is internally normalized to $^{146}Nd/^{144}Nd = 0.7219$, and the 2SD were reported. Processed JNdi-1 represents that the JNdi-1 standard, similar to the natural samples, was processed through our TODGA resin column and then measured by MC-ICP-MS.

indicates that no artificial Nd isotopic fractionation was introduced in column chemistry. Second, two geological materials, BHVO-2 and GSP-2, were used to check the effect of different sample types. The results show that the two rock standards with equivalent Nd loading (1 μg) both give similar patterns with the synthetic solutions (Fig. 2a) at our Nd section from 48 mL to 60 mL. It is noteworthy that this purification method was very sensitive to the molarity of HCl; thus, the molarity of HCl should be carefully calibrated by the standard NaOH solution before using it. The Nd fractions were measured for the matrix/Nd ratios using ICP-MS. As expected, the purified BHVO-2 and GSP-2 samples both have extremely low matrix/Nd ratios such as Na/Nd < 0.05, Mg/Nd < 0.04, Al/Nd < 0.05, K/Nd < 0.1, Ca/Nd < 0.05, Mn/Nd < 0.02, Fe/Nd < 0.05, Sr/Nd < 0.001, Ba/Nd < 0.02, La/Nd < 0.001, Ce/Nd < 0.001, Pr/Nd < 0.001, Sm/Nd < 0.001, and Eu/Nd < 0.001, indicating that our method is effective to purify Nd for natural samples. The whole procedure blank was diluted using 1 mL 2% HNO_3 and scanned for the ^{144}Nd signal. The result shows the intensity of ^{144}Nd less than 0.2 mV, which is equivalent to 27.4 pg Nd blanks. Third, the different Nd masses ranging from 2, 5 to 10 μg were loaded on the TODGA resin to test its effect. The result shows that all the Nd cuts overlap with each other in 12 mL 2 M HCl (Fig. 2b).

3.2 Assessing the Ce effect on $\delta^{142/144}Nd$

Due to the similar chemical properties of Ce and Nd, the ^{142}Ce isobaric interference on ^{142}Nd is always a concern in Nd isotope analyses. Previous studies confirmed that even a trace amount Ce could cause significant isotope offset on the Nd isotopic ratios.[13,17] To further assess the influence of Ce on Nd isotopic analysis in this study, different amounts of pure Ce were doped into 200 ng g^{-1} JNdi-1 standards to test the isobaric interferences of ^{142}Ce. As shown in Fig. 3, the $\delta^{142/144}Nd$ values bias significantly with the increase in the Ce/Nd ratios, indicating that interferences could not be removed *via* a simple mathematical correction when the Ce/Nd ratios exceeded 0.01. It is thus imperative to achieve efficient Ce–Nd separation for the accurate determination of stable Nd isotopic compositions in geological samples. As shown in Table 3, all the geological rocks used here through the Nd separation technique have $^{140}Ce/^{144}Nd$ ratios less than 0.00967, which is equal to the Ce/Nd ratios of 0.003, suggesting that Ce has little effect on our results.

3.3 Assessing the Eu effect on $\delta^{146/144}Nd$

The supersonic expansion of ions and space charge effects is widely acknowledged to be the main cause of mass bias within MC-ICP-MS.[30,43] The two processes are both directly related to the analyte compositions and concentrations. Therefore, it is essential to investigate the Eu effect on the determination of the Nd isotopic compositions. Concentrations ranging from 30 to
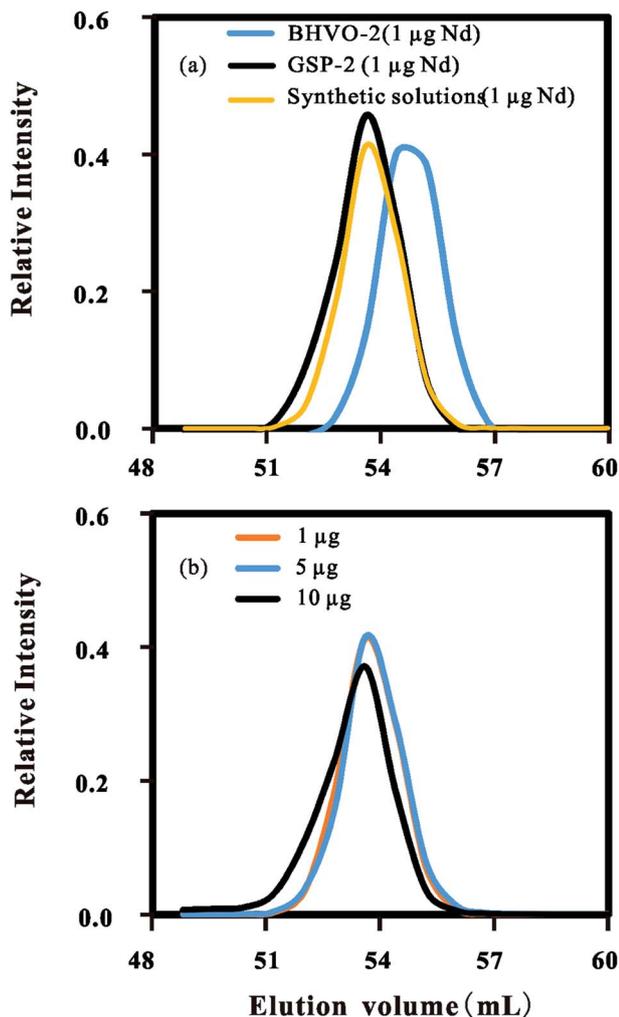
Fig. 2 Elution curves of Nd purification procedures using different rock standards (a) and masses of Nd loaded onto the 2 mL TODGA column (b). The matrix elements such as Ca, Sr, Fe, Ti, Al, La, and Ce are not shown in the plot as they were removed before adding 12 mL 2 M HCl.

70 ng g^{-1} pure Eu solutions were added into 200 ng g^{-1} JNdi-1 standards to select appropriate Eu concentration. The result showed that for the ^{153}Eu/^{143}Nd ratio (signal intensity) of 0.62, 0.81, 1.02, 1.22, and 1.47, the $\delta^{146/144}$Nd value (mean ± 2SD, $n =$ 20) was −0.006 ± 0.028‰, 0.001 ± 0.030‰, −0.003 ± 0.027‰, −0.003 ± 0.027‰, and 0.000 ± 0.031‰, respectively. The $\delta^{146/144}$Nd values did not deviate from the zero values when a series of solutions of various Eu/Nd ratios was tested. In this view, we selected the ^{153}Eu/^{143}Nd ratio of 1 throughout the whole analysis, which corresponds to about 48 ng g^{-1} Eu.

In order to better assess the influence of mismatching Eu concentration between the standards and the samples, La Jolla and Nd-GIG with the lowest and highest $\delta^{146/144}$Nd values, respectively, were tested by doping with different Eu contents. Fig. 4 shows the $\delta^{146/144}$Nd results of both La Jolla and Nd-GIG with different sample/standard Eu ratios. Along with the increasing sample/standard Eu ratios, the $\delta^{146/144}$Nd values of both La Jolla and Nd-GIG gradually decrease and bias from their
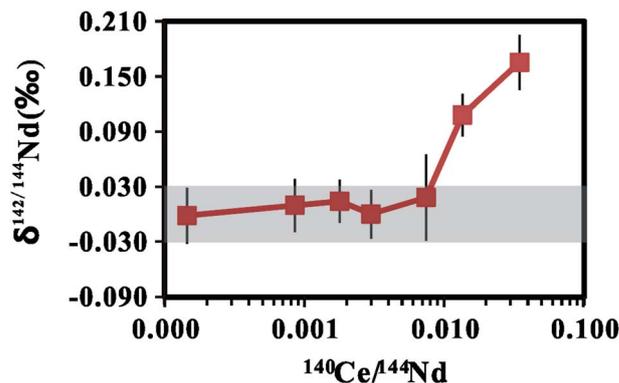
Fig. 3 The influence of ^{142}Ce isobaric interference on ^{142}Nd to the $\delta^{142/144}$Nd value for JNdi-1. The error bars (2SD) are based on four replicate measurements.

true values when the sample/standard Eu ratios are not in the adequate range. This indicates that the mass bias could not be accurately corrected even with a Eu internal standard if not adequately doped, similar to that with Zr for Sr.[43] As also presented in Fig. 4, both La Jolla and Nd-GIG are not bias from their ture values at the ±0.030‰ level when the Eu concentrations of the sample solution is within 10% difference of the standard solutions, which highlights the importance of matrix matching between the samples and the standards. Therefore, the concentrations of all the samples introduced into the
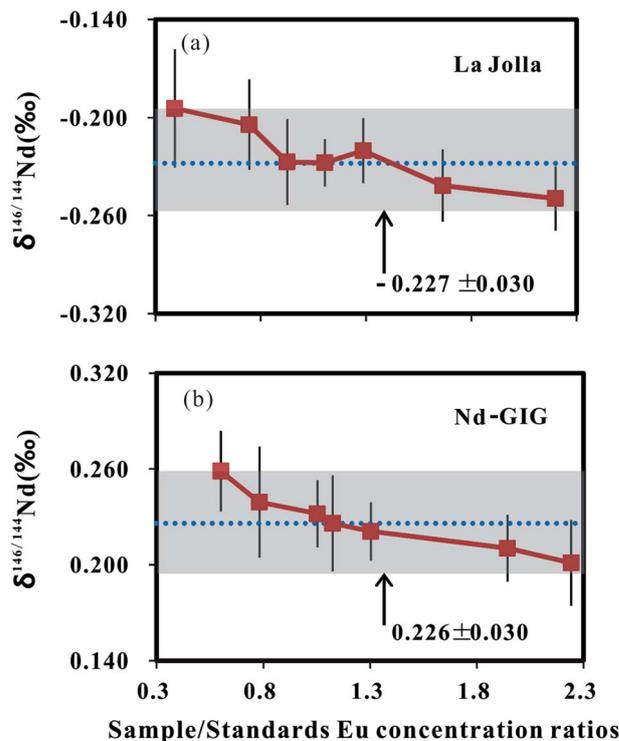

Fig. 4 Effect of Eu concentration on the measured $\delta^{146/144}$Nd values for La Jolla (a) and Nd-GIG (b), showing the need of matches between the samples and the standards within 10% difference. The error bars (2SD) are based on four replicate measurements.

2700 | J. Anal. At. Spectrom., 2021, 36, 2695–2703

This journal is © The Royal Society of Chemistry 2021

instruments were carefully adjusted to within 10% difference of the mix solutions, including 200 ng g^{-1} Nd and 48 ng g^{-1} Eu.

3.4 Precision and accuracy

The precision and accuracy of our method were assessed by comparing the results of SSB and C-SSBIN, and conducting replicated measurements of the standard samples, including pure Nd standards (JNdi-1, La Jolla, and Nd-GIG) and rock standards (BCR-1, BHVO-2, AGV-2, GSP-2, NOD-P-1, NOD-A-1, and GBW07249).

There is a clear improvement in the precision of the data when using Eu for mass bias correction. This was most striking for the repeat measurement of the JNdi-1 standards, which yielded $\delta^{146/144}$Nd = 0.006 ± 0.089‰ (2SD, n = 52) with only the SSB method but $\delta^{146/144}$Nd = 0.000 ± 0.029‰ (2SD, n = 60) using Eu as an internal standard in combination with SSB. Although this precision of the C-SSBIN results is slightly poorer than the precision of 0.017% measured by the DS-TIMS methodology,[10,15,16] it is still good enough to identify stable Nd isotopic fractionation occurring in geological processes.

Replicate measurements of both the pure Nd standards (JNdi-1, La Jolla, Nd-GIG) and rock standards indicate that Eu internal corrections not only improved the precision but also the accuracy. Long-term analyses of the JNdi-1 standard produced a total average $\delta^{142/144}$Nd of 0.000 ± 0.029‰ (2SD, n = 210), $\delta^{145/144}$Nd of 0.000 ± 0.029‰ (2SD, n = 210), and $\delta^{146/144}$Nd of 0.000 ± 0.027‰ (2SD, n = 210). International standard La Jolla was 0.230 ± 0.029‰ (2SD, n = 20), −0.114 ± 0.025‰ (2SD, n = 20), and −0.227 ± 0.030‰ (2SD, n = 20). Nd-GIG has an $\delta^{142/144}$Nd of −0.237 ± 0.025‰ (2SD, n = 20), $\delta^{145/144}$Nd of 0.105 ± 0.030‰ (2SD, n = 20), and $\delta^{146/144}$Nd of 0.226 ± 0.021‰ (2SD, n = 20). These results are in agreement with the values reported by the double-spike method (see Table 3).

In order to further assess the accuracy of our analytical protocol, the possessed JNdi-1 and rock standards (BHVO-2, BCR-1, AGV-2, and GSP-2) were measured in our laboratory (Table 3). The possessed JNdi-1 yield $\delta^{142/144}$Nd = −0.003 ± 0.029‰ (2SD, n = 6), $\delta^{145/144}$Nd = −0.006 ± 0.031‰ (2SD, n = 6), and $\delta^{146/144}$Nd = −0.007 ± 0.021‰ (2SD, n = 6), indicating that the chemical purification and instrument measurements did not cause artificial isotopic fractionations. Because of many stable Nd isotope terminologies reported in the literature, we cannot directly comprise our results with the previous works. Therefore, the published data were normalized to the $\delta^{146/144}$Nd values using the exponential law, namely, $\delta^{146/144}$Nd = −0.9865 × $\delta^{142/144}$Nd and $\delta^{146/144}$Nd = 1.9912 × $\delta^{145/144}$Nd, respectively. The $\delta^{146/144}$Nd (means ± 2SD, n = 4) of BHVO-2, BCR-1, AGV-2, and GSP-2 relative to JNdi-1 is −0.030 ± 0.030‰, −0.022 ± 0.030‰, −0.014 ± 0.030‰, and −0.063 ± 0.031‰, which is consistent with the results of the DS-TIMS methods within error (see Tables S1 and S3†), respectively.

3.5 Stable and radiogenic Nd isotopic compositions of the reference materials

Using the method developed herein, we measured seven widely used rock standards, including basalts (BHVO-2 and BCR-1),

andesite (AGV-2), granodiorite (GSP-2), and nodule samples (NOD-P-1, NOD-A-1, and GBW07249). All the matrix elements of the purified Nd solutions were strictly monitored using ICP-MS before Nd isotopic measurements. No detectable effect on any matrix elements such as Ca and isobaric elements such as Sm were found in purified Nd solutions. The values (means ± 2SD, n = 4) of $\delta^{142/144}$Nd, $\delta^{145/144}$Nd, and $\delta^{146/144}$Nd were 0.025 ± 0.045‰, −0.008 ± 0.031‰, and −0.030 ± 0.030‰ for BHVO-2; 0.033 ± 0.010‰, −0.007 ± 0.020‰, and −0.022 ± 0.030‰ for BCR-1; 0.010 ± 0.020‰, 0.004 ± 0.040‰, and −0.014 ± 0.030‰ for AGV-2; 0.054 ± 0.037‰, −0.028 ± 0.028‰, and −0.063 ± 0.031‰ for GSP-2, respectively. These results are in good agreement with the published DS-TIMS methods within the analytical uncertainties,[10,16] demonstrating the robustness of our methods (Table 3 and Fig. 5). To the best of our knowledge, no attempt has been made to study the nodule standards. NOD-P-1 has $\delta^{142/144}$Nd = 0.024 ± 0.033‰ (2SD, n = 4), $\delta^{145/144}$Nd = −0.004 ± 0.029‰ (2SD, n = 4), and $\delta^{146/144}$Nd = 0.002 ± 0.026‰ (2SD, n = 4); NOD-A-1 is 0.055 ± 0.052‰ (2SD, n = 4), −0.007 ± 0.021‰ (2SD, n = 4), and −0.015 ± 0.028‰ (2SD, n = 4); GBW07249 is 0.044 ± 0.036‰ (2SD, n = 4), −0.018 ± 0.010‰ (2SD, n = 4), and −0.030 ± 0.023‰ (2SD, n = 4).

The Nd three isotope plots for all pure Nd standards and rock standards are shown in Fig. 6. The slope of the $\delta^{142/144}$Nd and $\delta^{146/144}$Nd fractionation line is $Y = -1.0238X + 0.0049$ (R^2 = 0.9774), which is consistent with the kinetic (−1.0137) or equilibrium (−1.028) fractionation within analytical errors. Also, the slope of the $\delta^{145/144}$Nd and $\delta^{146/144}$Nd fractionation line
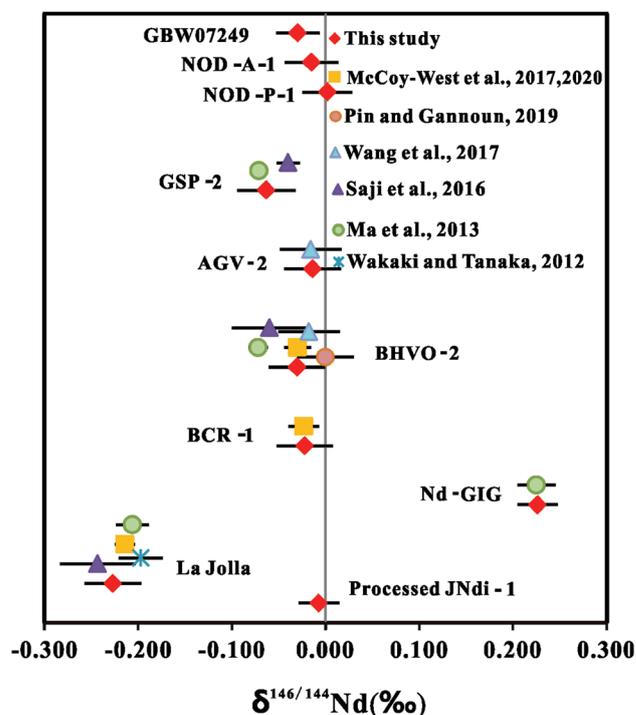

Fig. 5 Comparison of the $\delta^{146/144}$Nd values for international reference materials taken from Table 3.

This journal is © The Royal Society of Chemistry 2021

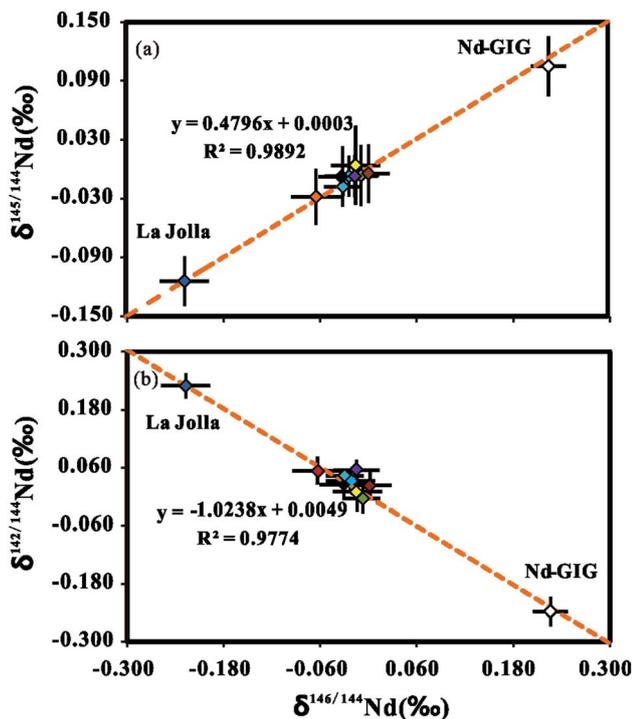*J. Anal. At. Spectrom.*, 2021, **36**, 2695–2703 | **2701**

Fig. 6 Neodymium (Nd) three isotope plot of all the samples. The samples analyzed in this study define a line with a slope of 0.4796 in the $\delta^{145/144}$Nd-$\delta^{146/144}$Nd mass fractionation line (a) and −1.0238 in the $\delta^{142/144}$Nd-$\delta^{146/144}$Nd mass fractionation line (b).
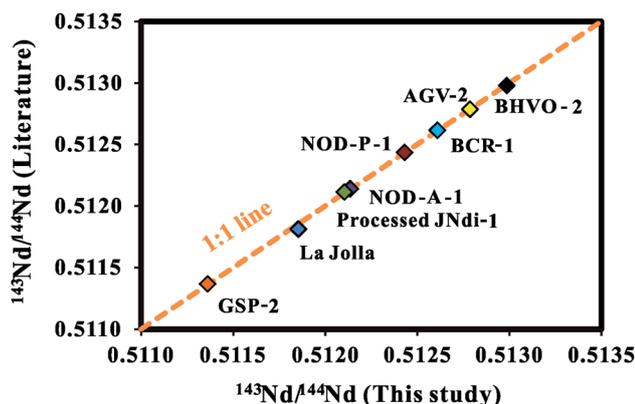

Fig. 7 Comparison results of radiogenic ^{143}Nd/^{144}Nd ratio. The literature ^{143}Nd/^{144}Nd ratios were taken from the preferred values reported in the GeoReM database (http://georem.mpch-mainz.gwdg.de/).

is $Y = 0.4796X + 0.0003$ ($R^2 = 0.9892$), consistent with the kinetic (0.5022) or equilibrium (0.5039) fractionation within error.

In addition to stable Nd isotopic compositions, our method also allows the concurrent determination of radiogenic ^{143}Nd/^{144}Nd ratio. The processed JNdi-1, La Jolla, and Nd-GIG yielded a radiogenic ^{143}Nd/^{144}Nd ratio of 0.512104 ± 8 (2SD, $n = 6$), 0.511856 ± 11 (2SD, $n = 20$), and 0.511512 ± 9 (2SD, $n = 20$), respectively. The geological standards yielded radiogenic ^{143}Nd/^{144}Nd ratios (2SD, $n = 4$) of 0.512609 ± 11 for BCR-1,

0.512987 ± 17 for BHVO-2, 0.512786 ± 10 for AGV-2, 0.511361 ± 9 for GSP-2, 0.512432 ± 14 for NOD-P-1, 0.512136 ± 5 for NOD-A-1, and 0.512334 ± 12 for GBW07249, respectively. These results are in good agreement with the preferred values reported in the GeoReM Database (http://georem.mpch-mainz.gwdg.de/) (Table 3 and Fig. 7).

4. Conclusions

A practical method for the simultaneous measurement of the stable and radiogenic Nd isotopic ratio was developed in this study. Using a single-step TODGA resin column, the perfect separation of Nd from Ce, Pr, and Sm with nearly 100% Nd yield and low procedural blanks (<50 pg) was achieved. Combined standard-sampled bracketing and Eu internal normalization isotopic fractionation correction model gave an approximate 3-fold improvement in the precision of $\delta^{146/144}$Nd compared to that of only the SSB method. In addition, the factors affecting stable Nd isotopic analysis such as isobaric interferences and the effect of Eu on the δ-values were systematically tested and rigorously examined. The Ce/Nd ratios should be less than 0.01 for high precision Nd isotopic analysis measured by MC-ICP-MS. No discernible effect on the $\delta^{146/144}$Nd values was found when the difference in the sample-standard Eu concentrations is less than 10%. Based on repeated measurements of international standard JNdi-1, the long-term external precision of $\delta^{146/144}$Nd is better than ±0.030‰. Using our method, stable and radiogenic Nd isotopic compositions of a series of reference materials were obtained simultaneously, which is in good agreement with those given by the double-spike method.

Author contributions

J.-H. Bai, F. Liu, Z.-F. Zhang, G.-J. Wei conceived the study. J.-H. Bai performed the experiments. F. Liu, Y.-F. Liu, J.-L Ma, S.-X. Zhong contributed to the column chemistry. L. Zhang, J.-L. Ma contributed to the isotopic analysis. J.-H. Bai, F. Liu, G.-J. Wei analyzed the data. J.-H. Bai and F. Liu wrote the manuscript with significant input from all co-authors.

Conflicts of interest

The authors declare no competing financial interest.

Acknowledgements

References

1 M. Berglund and M. E. Wieser, *Pure Appl. Chem.*, 2011, **83**, 397–410.

2 D. J. DePaolo, Neodymium isotope geochemistry, *Minerals and Rocks*, Springer-Verlag, 1988.

3 R. E. Carlson, M. Boyet and M. Horan, *Science*, 2007, **316**, 1175–1178.

4 C. Burkhardt, L. E. Borg, G. A. Brennecka, Q. R. Shollenberger, N. Dauphas and T. Kleine, *Nature*, 2016, **537**, 394–398.

5 A. Gannoun, M. Boyet, H. Rizo and A. El Goresy, *Proc. Natl. Acad. Sci. U. S. A.*, 2011, **108**, 7693–7697.

6 F. Moynier, Q. Z. Yin, K. Irisawa, M. Boyet, B. Jacobsen and M. T. Rosing, *Proc. Natl. Acad. Sci. U. S. A.*, 2010, **107**, 10810–10814.

7 D. Vance and K. Burton, *Earth Planet. Sci. Lett.*, 1999, **173**, 365–379.

8 C. Jeandel, T. Arsouze, F. Lacan, P. Téchiné and J. C. Dutay, *Chem. Geol.*, 2007, **239**, 156–164.

9 T. Arsouze, J. C. Dutay, F. Lacan and C. Jeandel, *Chem. Geol.*, 2007, **239**, 165–177.

10 A. J. McCoy-West, M.-A. Millet and K. W. Burton, *Earth Planet. Sci. Lett.*, 2017, **480**, 121–132.

11 X. Liu, G. J. Wei, J. Q. Zou, Y. R. Guo, J. L. Ma, X. F. Chen, Y. Liu, J. F. Chen, H. L. Li and T. Zeng, *J. Geophys. Res.: Oceans*, 2018, **123**, 9137–9155.

12 A. J. McCoy-West, M.-A. Millet and K. W. Burton, *Front. Earth Sci.*, 2020b, **8**.

13 J. L. Ma, G. J. Wei, Y. Liu, Z. Y. Ren, Y. G. Xu and Y. H. Yang, *J. Anal. At. Spectrom.*, 2013, **28**, 1926–1931.

14 A. J. McCoy-West, K. W. Burton, M.-A. Millet and P. A. Cawood, *Geochim. Cosmochim. Acta*, 2021, **293**, 575–597.

15 S. Wakaki and T. Tanaka, *Int. J. Mass Spectrom.*, 2012, **323/324**, 45–54.

16 A. J. McCoy-West, M.-A. Millet, G. M. Nowell, O. Nebel and K. W. Burton, *J. Anal. At. Spectrom.*, 2020a, **35**, 388–402.

17 Y. Wang, X. Huang, Y. Sun, S. Zhao and Y. Yue, *Anal. Methods*, 2017, **9**, 3531–3540.

18 N. S. Saji, D. Wielandt, C. Paton and M. Bizzarro, *J. Anal. At. Spectrom.*, 2016, **31**, 1490–1504.

19 T. Ohno and T. Hirata, *Anal. Sci.*, 2013, **29**, 47–53.

20 C. Pin and A. Gannoun, *J. Anal. At. Spectrom.*, 2019, **34**, 310–318.

21 E. Hyung and F. L. H. Tissot, *J. Anal. At. Spectrom.*, 2021, **36**, 1946–1959.

22 M. Garçon, M. Boyet, R. W. Carlson, M. F. Horan, D. Auclair and T. D. Mock, *Chem. Geol.*, 2018, **476**, 493–514.

23 A. Retzmann, T. Zimmermann, D. Profrock, T. Prohaska and J. Irrgeher, *Anal. Bioanal. Chem.*, 2017, **409**, 5463–5480.

24 Z.-Y. Chu, M.-J. Wang, C.-F. Li, Y.-H. Yang, J.-J. Xu, W. Wang and J.-H. Guo, *J. Anal. At. Spectrom.*, 2019, **34**, 2053–2060.

25 M. Willig and A. Stracke, *Chem. Geol.*, 2018, **476**, 119–129.

26 Y. J. An, F. Wu, Y. X. Xiang, X. Y. Nan, X. Yu, J. H. Yang, H. M. Yu, L. W. Xie and F. Huang, *Chem. Geol.*, 2014, **390**, 9–21.

27 X. Y. Nan, F. Wu, Z. F. Zhang, Z. H. Hou, F. Huang and H. M. Yu, *J. Anal. At. Spectrom.*, 2015, **30**, 2307–2315.

28 S. Klemme, J. D. Blundy and B. J. Wood, *Geochim. Cosmochim. Acta*, 2002, **66**, 3109–3123.

29 G. L. Arnold, S. Weyer and A. D. Anbar, *Anal. Chem.*, 2004, **76**, 322–327.

30 L. Yang, S. Tong, L. Zhou, Z. Hu, Z. Mester and J. Meija, *J. Anal. At. Spectrom.*, 2018, **33**, 1849–1861.

31 D. Vance and M. Thirlwall, *Chem. Geol.*, 2002, **185**, 227–240.

32 G. Wu, J. M. Zhu, X. Wang, T. M. Johnson and G. Han, *Anal. Chem.*, 2020, **92**, 1463–1469.

33 X. K. Zhu, Y. Guo, R. K. O'Nions, E. D. Young and R. D. Ash, *Nature*, 2001, **412**, 311–313.

34 X. He, J. Ma, G. Wei, L. Zhang, Z. Wang and Q. Wang, *J. Anal. At. Spectrom.*, 2020, **35**, 100–106.

35 L. P. Feng, L. Zhou, L. Yang, W. Zhang, Q. Wang, S. Y. Tong and Z. C. Hu, *J. Anal. At. Spectrom.*, 2018, **33**, 413–421.

36 J. E. Roe, A. D. Anbar and J. Barling, *Chem. Geol.*, 2003, **195**, 69–85.

37 A. D. Anbar, K. A. Knab and J. Barling, *Anal. Chem.*, 2001, **73**, 1425–1431.

38 W. M. White, F. Albarède and P. Télouk, *Chem. Geol.*, 2000, **167**, 257–270.

39 M. Dayah, *Periodic Table-Ptable*, 1 Oct. 1997, https://ptable.com.

40 T. L. Chang, Q. Y. Qian, M. T. Zhao and J. Wang, *Int. J. Mass Spectrom. Ion Processes*, 1994, **139**, 95–102.

41 A. Pourmand and N. Dauphas, *Talanta*, 2010, **81**, 741–753.

42 Q. Guan, Y. Sun, Y. Yue, X. Liu and S. Zhao, *Anal. Sci.*, 2019, **35**, 323–328.

43 L. Yang, C. Peter, U. Panne and R. E. Sturgeon, *J. Anal. At. Spectrom.*, 2008, **23**, 1269.

This journal is © The Royal Society of Chemistry 2021

J. Anal. At. Spectrom., 2021, **36**, 2695–2703 | **2703**